A Novel B7-H6–Targeted IgG-Like T Cell–Engaging Antibody for the Treatment of Gastrointestinal Tumors

Wei Zhang[1], Aurélie Auguste[2], Xiaoyun Liao[3], Christian Walterskirchen[4], Kathrin Bauer[4], Yu-Hsi Lin[1], Ling Yang[1], Farzaneh Sayedian[5], Markus Fabits[6], Michael Bergmann[6], Carina Binder[7], Leticia Corrales[4], Anne B. Vogt[4], Lindsey J. Hudson[8], Martin P. Barnes[8], Arnima Bisht[9], Craig Giragossian[10], Vladimir Voynov[10], Paul J. Adam[4], and Susanne Hipp[1,11]

ABSTRACT

Purpose: Advanced-stage gastrointestinal cancers represent a high unmet need requiring new effective therapies. We investigated the antitumor activity of a novel T cell–engaging antibody (B7-H6/CD3 ITE) targeting B7-H6, a tumor-associated antigen that is expressed in gastrointestinal tumors.

Experimental Design: Membrane proteomics and IHC analysis identified B7-H6 as a tumor-associated antigen in gastrointestinal tumor tissues with no to very little expression in normal tissues. The antitumor activity and mode of action of B7-H6/CD3 ITE was evaluated in *in vitro* coculture assays, in humanized mouse tumor models, and in colorectal cancer precision cut tumor slice cultures.

Results: B7-H6 expression was detected in 98% of colorectal cancer, 77% of gastric cancer, and 63% of pancreatic cancer tissue samples. B7-H6/CD3 ITE-mediated redirection of T cells toward B7-H6–positive tumor cells resulted in B7-H6–dependent lysis of tumor cells, activation and proliferation of T cells, and cytokine secretion in *in vitro* coculture assays, and infiltration of T cells into tumor tissues associated with tumor regression in *in vivo* colorectal cancer models. In primary patient-derived colorectal cancer precision-cut tumor slice cultures, treatment with B7-H6/CD3 ITE elicited cytokine secretion by endogenous tumor-infiltrating immune cells. Combination with anti-PD-1 further enhanced the activity of the B7-H6/CD3 ITE.

Conclusion: These data highlight the potential of the B7-H6/CD3 ITE to induce T cell–redirected lysis of tumor cells and recruitment of T cells into noninflamed tumor tissues, leading to antitumor activity in *in vitro, in vivo*, and human tumor slice cultures, which supports further evaluation in a clinical study.

Introduction

Gastrointestinal cancers including colorectal, gastric, and pancreatic cancer remain a leading cause of cancer-related deaths in both men and women worldwide with more than 900,000, 760,000, and 466,000 deaths, respectively, every year (1–3).

Bispecific T-cell engagers represent a promising class of antibody-based cancer immunotherapy. These biotherapeutics are designed to facilitate the formation of a cytolytic synapse by binding concomitantly to an antigen on the tumor cells and to CD3 on T cells and direct the cytolytic activity of the T cells selectively to the tumor cells. After formation of the cytolytic synapse, the T cells increase the secretion of perforin and granzyme B, resulting in apoptosis of the tumor cells. Subsequent activation and proliferation of T cells leads to transient release of cytokines, which attracts other immune cells to the tumor tissue and has the potential to broaden the immune response against the tumor cells and convert a noninflamed (cold) into an inflamed (hot) tumor environment (4–9). While the first bispecific T-cell engagers targeted mostly lineage antigens in hematologic cancers and utilized the short half-life BiTE format which was administered via continuous intravenous infusion (10, 11), the next generation of T-cell engagers are based on bispecific formats incorporating half-life extension for increased dosing convenience and target novel antigens on solid tumors (6, 8, 9, 12–16). After the successful development of T cell–engaging therapies in hematologic tumors (10, 11), the proof of principle for treatment of patients with solid tumors was demonstrated only recently. In a phase III trial, treatment of patients with metastatic uveal melanoma with tebentafusp, an HLA-A*02:01/gp100/CD3 ImmTAC molecule, led to longer overall survival compared with the control group and was recently approved by the FDA (17).

However, for gastrointestinal tumors, the identification of tumor-associated antigens to ensure a therapeutic window remains challenging. In a phase I clinical trial with solitomab, an EpCAM targeting BiTE, in patients with solid tumors, treatment was associated with dose-limiting toxicities including severe diarrhea and increased liver enzymes, which is most likely associated to the expression of EpCAM in various healthy epithelial tissues including colon, small intestine, and hepatoblasts (18, 19). Treatment with MEDI-565, a BiTE targeting

[1]Boehringer Ingelheim Pharmaceuticals, Inc., Cancer Immunology & Immune Modulation, Ridgefield, Connecticut. [2]Boehringer Ingelheim Pharma, GmbH & Co KG, Translational Medicine and Clinical Pharmacology, Biberach an der Riß, Germany. [3]Boehringer Ingelheim Pharmaceuticals, Inc., Oncology Translational Science, Ridgefield, Connecticut. [4]Boehringer Ingelheim RCV, GmbH & Co KG., Cancer Immunology & Immune Modulation, Vienna, Austria. [5]Roche Tissue Diagnostics, Tucson, Arizona. [6]Medical University of Vienna, Division of Visceral Surgery, Department of General Surgery and Comprehensive Cancer Center, Vienna, Austria. [7]Department of Pathology, Medical University of Vienna, Vienna, Austria. [8]Oxford BioTherapeutics, Ltd., Oxon, United Kingdom. [9]Oxford BioTherapeutics, Inc., San Jose, California. [10]Boehringer Ingelheim Pharmaceuticals, Inc., Biotherapeutics Discovery, Ridgefield, Connecticut. [11]Boehringer Ingelheim Pharmaceuticals, Inc., Translational Medicine and Clinical Pharmacology, Ridgefield, Connecticut.

Prior presentation: Parts of this study have been presented at the AACR Annual Meeting 2021.

Corresponding Author: Susanne Hipp, Translational Medicine & Clinical Pharmacology, Boehringer Ingelheim Pharmaceuticals, Inc., 900 Ridgebury Road, P.O. Box 368, Ridgefield, CT 06877-0368. Phone: 203-798-4567; E-mail: susanne.hipp@boehringer-ingelheim.com

Clin Cancer Res 2022;28:5190–201

doi: 10.1158/1078-0432.CCR-22-2108

Translational Relevance

Current treatment options for gastrointestinal cancers mainly include chemotherapy-based regimens, and available targeted and immunotherapy options provide only insufficient antitumor responses. T-cell engagers represent tumor-targeted immunotherapies that utilize the cytolytic potential of T cells by selectively redirecting them toward tumor cell antigens, resulting in lysis of tumor cells. This article describes the discovery of B7-H6 as a tumor-associated antigen expressed at high prevalence in colorectal, gastric, and pancreatic cancer tissue, and provides mechanistic insights into the mode of action of a novel B7-H6–targeted IgG-like T cell–engaging antibody (B7-H6/CD3 ITE). In our studies, we show that the B7-H6/CD3 ITE efficiently redirects the cytolytic activity of T cells to B7-H6–positive tumor cells in *in vitro* and *in vivo* models as well as patient-derived colorectal cancer precision-cut tumor slice cultures. The tumor selectivity and antitumor activity of the B7-H6/CD3 ITE support the ongoing clinical trial in patients with B7-H6–positive cancers.

CEA, in a phase I trial in patients with gastrointestinal adenocarcinomas also led to dose-limiting toxicities including diarrhea and cytokine release syndromes which precluded dose escalation to therapeutic levels (20), very likely due to the expression of CEA in healthy tissues of the gastrointestinal organs (21).

In this article, we describe the identification of B7-H6 (NCR3LG1), a member of the B7 family of immune receptors which has been previously described to play a role in natural killer (NK) cell–mediated cytotoxicity (22–24), as a novel tumor-associated antigen in gastrointestinal tumors and the preclinical characterization of a novel half-life extended B7-H6–targeted IgG-like T-cell engager (ITE). B7-H6/CD3 ITE monotherapy treatment induces potent and strictly B7-H6–dependent lysis of tumor cells and infiltration of T cells into the tumor tissue resulting in tumor regression and an inflamed tumor environment. The activity was further enhanced when combined with anti-PD-1 treatment. The B7-H6/CD3 ITE (BI 765049) is currently being investigated in a nonrandomized, open-label, dose-escalation trial as monotherapy and in combination with anti-PD-1 (ezabenlimab; ref. 25) in patients with B7-H6–expressing tumors (NCT04752215; ref. 26).

Materials and Methods

Human peripheral blood mononuclear cells and tissues

Fresh buffy coats from healthy volunteers were obtained from the Austrian Red Cross or HemaCare. Human tissues were obtained from the Department of Pathology at the Medical University of Vienna, Austria, or Indivumed GmbH. All blood donors and patients provided written informed consent in accordance with the Declaration of Helsinki and the studies were approved by the Institutional Review Board before sample collection.

Proteomic analysis of tumor and normal (noncancerous) tissues

Plasma membrane fractionations were isolated and analyzed by LC/MS as described previously (27). Obtained raw data were processed compared with the OGAP (Oxford Genome Anatomy Project, Oxford Biotherapeutics) platform. The OGAP platform was built on integrating experimental proteomics data together with molecular, cellular, phenotypic, and clinical information and is designed to allow rapid characterization and identification of proteins in human tissue samples (28).

IHC analysis

B7-H6

Tissue sections were stained with anti-B7-H6 antibody (Ventana Medical Systems) or negative control followed by OptiView DAB IHC Detection Kit on the BenchMark ULTRA automated system (all reagents and platform from Ventana Medical Systems). The stained tissue sections were evaluated by a trained pathologist and sections containing at least 1% B7-H6–expressing tumor cells were scored as positive. B7-H6 staining intensity was scored as 1+ (weak), 2+ (moderate), and 3+ (strong). H-score = 3 × percentage of strong-positive cells + 2 × percentage of moderate-positive cells + percentage of weak-positive cells.

CD3, CD69, granzyme B, perforin, PD-L1, and cleaved caspase 3

Xenograft tumor tissues were stained with anti-human CD3 (Ventana, RRID:AB_2335978), anti-human CD69 (Abcam, RRID:AB_2922929), anti-granzyme B (Abcam, RRID:AB_2860567), anti-perforin (Leica Biosystems, RRID:AB_563955), anti-human PD-L1 (Leica Biosystems, RRID:AB_10555292), or anti-human cleaved caspase 3 (Cell Signaling Technology, RRID:AB_2070042) antibodies. Stained slides were scanned for digital quantitative analysis of CD3, CD69, granzyme B, perforin, and cleaved caspase 3 expression. PD-L1 staining was manually scored under a light microscope according to the following scoring system: 0: no membrane staining; 1+: a faint/barely perceptible membrane staining, the cells exhibit incomplete membrane staining; 2+: a weak to moderate complete membrane staining; 3+: a strong complete membrane staining. H-score was calculated as described above.

Engineering, expression, and purification of B7-H6/CD3 ITE

Antibodies cross-reactive to human and cynomolgus monkey B7-H6 were generated by single B-cell technology from AJ mice immunized with the recombinant extracellular domains of human and cynomolgus monkey B7-H6. Humanization and further sequence optimization of both variable regions was performed using a Fab expression vector system according to methods described previously (29). The murine anti-CD3 antibody described previously (30) was the source of the anti-CD3 binder used in the B7-H6/CD3 ITE. The B7-H6/CD3 ITE cross-reacts to human and cynomolgus monkey but not to rodent CD3. Subsequently, the optimized variable regions were formatted in an ITE expression construct, a two-chain heterodimeric bispecific antibody with Fab domains that contain polypeptide linkers to assure correct light-heavy chain pairing and an Fc domain engineered for heterodimerization and efficient purification (31), using a pTT5 expression vector (National Research Council, Canada) with common molecular biology techniques. The B7-H6/CD3 ITE was produced in CHO-E (National Research Council) cells by transient transfection. After 10 days of culturing, the supernatant was harvested and purified by Protein A affinity chromatography using MabSelect columns (GE Healthcare). The bispecific antibody was further purified by cation exchange chromatography using a Poros 50 HS column (Applied Biosystems) and stored in 50 mmol/L sodium acetate and 100 mmol/L NaCl, pH 5.0 buffer. Analytic characterization by intact mass spectrometry, SDS-PAGE, and size-exclusion chromatography showed that the purified antibody has the expected heterodimeric mass and contained minimal high molecular weight aggregate (less than 1%) and no contaminating homodimeric species.

Cell lines and cell culture

NCI-H716 (CCL-251, RRID:CVCL_1581), HCT-15 (CCL-225, RRID:CVCL_0292), HT-29 (HTB-38, RRID:CVCL_0320), LoVo (CCL-229, RRID:CVCL_0399), RKO-E6 (CRL-2578, RRID:CVCL_3787), HCI-H508 (CCL-253, RRID:CVCL_1564), Colo201 (CCL-224, RRID:CVCL_1987), SNU-C1 (CRL-5972, RRID:CVCL_1708), LS411N (CRL-2159, RRID:CVCL_1385), AGS (CRL-1739, RRID:CVCL_0139), SNU-16 (CRL-5974, RRID:CVCL_0076), HS746T (HTB-135, RRID:CVCL_0333), Capan-1 (HTB-79, RRID:CVCL_0237), SW1990 (CRL2172, RRID:CVCL_1723), Panc 02.13 (CRL-2554, RRID:CVCL_1634), AsPC-1 (CRL-1682, RRID:CVCL_0152), Panc 03.27 (CRL-2549, RRID:CVCL_1635), Panc-1 (CRL-1469, RRID:CVCL_0480), CFPAC-1 (CRL-1918, RRID:CVCL_1119), HPAFF-II (CRL-1997, RRID:CVCL_0313) were purchased from the ATCC. MKN-45 (ACC 409, RRID:CVCL_0434), 23132/87 (ACC 201, RRID:CVCL_1046), PA-TU-8988T (ACC 162, RRID:CVCL_1847), and HuPT4 (ACC 233, RRID:CVCL_1300) were purchased from the German Collection of Microorganisms and Cell Cultures (DSMZ). SNU-C4 (0000C4.1, RRID:CVCL_5111) and SNU-719 (00719.1, RRID:CVCL_5086) were purchased from the Korean Cell Line Bank (KCLB). NUGC-3 (JCRB0822, RRID:CVCL_1612), OCUM-1 (JCRB0172, RRID:CVCL_3084), NCC-StC-K140 (JCRB1228, RRID:CVCL_3055), KP-3 (JCRB0178.0, RRID:CVCL_3005), SUIT-2 (JCRB1094, RRID:CVCL_3172) were purchased from the Japanese Collection of Research Bioresources (JCRB). MKN74 (TCB1002, RRID:CVCL_2791) was purchased from RIKEN BRC Cell Bank. All cell lines were cultured according to supplier's (ATCC, KCLB, DSMZ, JCRB, RIKEN BRC cell bank) instruction. The recombinant PD-L1 overexpression cell line HCT-15-PD-L1 was generated by lentiviral transduction. Lentivirus was generated using a PD-L1 (Uniprot, #Q9NZQ7) encoding plasmid in 293FT cells (Thermo Fisher Scientific). All cell lines were tested to exclude *Mycoplasma* contamination and maintained in culture for a maximum of 20 passages.

Isolation of peripheral blood mononuclear cells and T cells

Peripheral blood mononuclear cells (PBMC) were purified from buffy coats by density gradient centrifugation. T-cell subsets were purified from PBMCs using the respective T-cell subset isolation kits (Miltenyi Biotec) according to manufacturer's instructions.

Quantification of B7-H6 cell surface molecules on cell lines

Quantification of B7-H6 and PD-L1 cell surface molecules expressed on cancer cell lines was performed by flow cytometry using the QIFIKIT (Agilent) according of manufacturer's instructions.

Cytotoxicity, T-cell activation, T-cell proliferation, cytokine secretion assays

Cytotoxicity, activation, degranulation, and proliferation of T cells, and cytokine secretion were analyzed in multiparametric cytotoxicity assays. Cell lysis was assessed by quantification of lactate dehydrogenase concentrations in the cell culture supernatant using the Cytotoxicity Detection Kit^{PLUS} (Sigma-Aldrich) according to manufacturer's instructions. Activation and degranulation of T cells were assessed by staining cells for extracellular CD25 (anti-CD25-APC, Becton Dickinson, RRID:AB_2916552), CD69 (anti-CD69-PE-Cy7, Becton Dickinson, RRID:AB_396851), and CD107a (anti-CD107a-BV421, BioLegend, RRID:AB_11203537), and intracellular granzyme B (anti-GrzB-FITC, Becton Dickinson, RRID:AB_1645488) by flow cytometry. For analysis of T-cell proliferation, the PBMCs were labeled with CFDA-SE (Becton Dickinson) and T cells were additionally stained with anti-CD3 (BioLegend, RRID:AB_2561628). Cytokine concentrations were analyzed from supernatants of cytotoxicity assays using the V-PLEX Assays (Mesoscale Discovery) following the manufacturer's instructions.

Mouse xenograft studies

All animal studies were approved by the respective Institutional Animal Care and Use Committees (IACUC). Antitumor activity was evaluated in female HCT-15 and HCT-15-PD-L1 xenograft bearing PBMC-humanized NOD.Cg-*Prkdc*^{scid} *Il2rg*^{tm1Wjl}/SzJ (NSG, RRID:IMSR_JAX:005557), and NCI-H716 xenograft bearing T cell–humanized NOD.Cg-*Prkdc*^{scid}*Il2rg*^{tm1Sug}/JicTac (NOG, RRID:IMSR_TAC:HSCFTL-NOG) mice.

NOG mice were irradiated (200 Rad) the day before NCI-H716 cell injection. A total of 2.5×10^7 HCT-15 or NCI-H716 or 1×10^7 HCT-15-PD-L1 cells suspended in 100 µL PBS were injected subcutaneously into the right flank of the animals at the timepoints outlined in the respective figures. For the T cell–humanized NOG model, T cells were isolated (Miltenyi Biotec #130-096-535) and expanded (Miltenyi Biotec, #130-091-441) for 17 days before intraperitoneal injection. PBMCs were injected intravenously as indicated in the respective figure. Animals were randomized into treatment groups based on tumor size one day before start of treatment. Tumor size was measured by an electronic caliper and calculated according to the formula "tumor volume = length*diameter^{2}*π/6". Regressions were defined as a relative tumor volume < 1 when normalized to the tumor volume before the start of treatment. Tumor growth inhibition was calculated according to the formula "% TGI = 100*(1-(MedianTx - MedianT0)/(MedianCx - MedianC0))" (Tx, T0 = tumor volume of B7-H6 ITE–treated group at timepoint x or 0; Cx, C0: tumor volume of vehicle group at timepoint x or 0).

Flow cytometry analysis of xenograft tumor tissues

For flow cytometry analysis of tumor tissues, tumors were harvested at the study end and dissociated using the human tumor dissociation kit (Miltenyi Biotec #130-095-929) following the manufacturer's instructions. After staining single-cell suspensions with fixable violet dead cell stain kit (Becton Dickinson #L34955) and subsequent blocking with anti-CD16/32 antibody (BioLegend, RRID:AB_2922498), cells were stained with anti-mouse CD45-FITC (clone 30F11, BioLegend, RRID:AB_312973), anti-human CD4-Alexa700 (clone RPA-T4, BioLegend, RRID:AB_493743), anti-human CD8-PE-Cy7 (clone T8, BioLegend, RRID:AB_2044007), anti-human CD19-BV650 (clone HIB19, BioLegend, RRID:AB_11126981), anti-human CD3-BUV737 (clone SK7, BD Biosciences, RRID:AB_2870083), and anti-human CD45-APC-H7 (clone 2D1, BD Biosciences, RRID:AB_1645734).

Pharmacokinetic studies

All animal studies were approved by the IACUC. Serum concentrations of B7-H6/CD3 ITE were determined in an ELISA-based assay using recombinant human B7-H6 (extracellular domain) protein as capture and human CD3εγ (Fc-fusion protein) as detection reagents. Data were treated as a naïve pool and fitted to a linear two-compartment model using Phoenix 64 WinNonlin 8.2 (Certara) and NONMEM7.4 (ICON Clinical Research).

Colorectal cancer precision-cut tumor slice cultures

Freshly excised tumor tissue was transferred to the lab within 30 minutes after surgery. Subsequently, 200 µmol/L sections were prepared using a Compresstome VF-300-0Z and incubated at 37°C, 5% CO_2 for 48 hours in DMEM 4.5 g/L D-glucose supplemented with 1x GlutaMAX, 1x Penicillin/Streptomycin/Amphotericin B, and 10% FCS in presence of 15 µg/mL B7-H6/CD3 ITE or medium alone.

B7-H6 and CD3 expression were analyzed by IHC in a tissue section that was taken at baseline, fixed in formalin and embedded in paraffin. IFNγ, IP-10, and IL2 were quantified in the cell supernatant using U-PLEX Assays (Mesoscale Discovery, #K15049K) following the manufacturer's instructions. Cytokines were quantified from all biological replicates, the mean value of each sample was then normalized to the respective untreated (medium only) samples and depicted as fold change.

Statistical analysis

Statistical analysis was performed using GraphPad Prism 9.0.0 software (RRID:SCR_002798). In experiments with two groups, a one-sided nonparametric Mann–Whitney *U* test was applied to compare the B7-H6/CD3 ITE-treated group to the vehicle-treated group. In experiments with more than two groups, a nonparametric one-way ANOVA test was applied to compare the B7-H6/CD3 ITE-treated groups with the respective vehicle-treated groups. ****, $P < 0.0001$; ***, $P < 0.001$; **, $P < 0.01$; *, $P < 0.05$.

Data availability statement

The data generated in this study are available within the article and its Supplementary Data. Raw data are available only upon reasonable request to comply with the patients' informed consent.

Results

B7-H6 expression in human colorectal, gastric, and pancreatic cancer tissues

We identified B7-H6 as a tumor-associated membrane protein in a proteomics screen using the OGAP proteomic discovery platform, where B7-H6 was detected in tumor tissue samples but not in any normal (noncancerous) tissues (Supplementary Fig. S1A). Analysis of The Cancer Genome Atlas datasets showed elevated expression levels of B7-H6 mRNA in gastrointestinal tumors including colorectal, gastric, and pancreatic cancer tissues (Supplementary Fig. S1B). The membranous B7-H6 expression pattern in tumor tissues was analyzed by IHC. In a pre-experiment, formalin-fixed and paraffin-embedded (FFPE) cell pellets from eight representative pancreatic cancer cell lines, covering the expression range from 90 to 13,000 B7-H6 molecules per cell on the cell surface (as determined by flow cytometry), were analyzed by IHC and membranous B7-H6 expression was detectable in cell pellets with approximately 600 or more B7-H6 molecules per cell, and the intensity correlated with the B7-H6 cell surface density (Supplementary Fig. S2). Subsequently, the membranous protein expression pattern of B7-H6 was analyzed in colorectal ($n = 50$; **Fig. 1A** and **B**), gastric ($n = 43$; **Fig. 1C** and **D**), and pancreatic cancer ($n = 46$; **Fig. 1E** and **F**) tissue samples. B7-H6 expression was detected in 98% of colorectal cancer, 77% of gastric cancer, and 63% of pancreatic cancer samples. H-scores ranged from 13 to 180 in colorectal cancer, 1 to 160 in gastric cancer, and 2 to 130 in pancreatic carcinoma samples. Expression of B7-H6 was independent of cancer stage.

Discovery and *in vitro* activity of B7-H6/CD3 ITE

The B7-H6/CD3 ITE is an ITE based on a bispecific heterodimeric IgG-like scaffold with monovalent binding to each antigen that incorporates flexible peptide linkers between light and heavy chains and is designed to bind concurrently to B7-H6 on tumor cells and CD3 on T cells while maintaining an IgG-like architecture (**Fig. 2A**). In a flow cytometry–based assessment using B7-H6–positive HCT-15 cells and CD3-positive human T cells, the B7-H6/CD3 ITE bound with an EC_{90} of 7 nmol/L to HCT-15 cells and 11 nmol/L to T cells (**Fig. 2B** and **C**). Furthermore, the B7-H6/CD3 ITE does not interfere in the natural interaction of B7-H6 and its ligand NKp30, and the consequential B7-H6–dependent activation of NK cells (Supplementary Fig. S3).

Initial characterization of B7-H6/CD3 ITE-mediated T cell–redirected tumor cell lysis was performed in coculture assays with human T cells and a panel of colorectal cancer, gastric, and pancreatic cancer cell lines, with B7-H6 cell surface expression levels ranging from 15 to 13,000 B7-H6 molecules per cell, and a fixed concentration of 1.5 μg/mL B7-H6/CD3 ITE. In these assays, the B7-H6/CD3 ITE induced lysis of colorectal cancer, gastric, and pancreatic cancer cell lines and the lysis activity correlated with the expression level of B7-H6 on the cell surface (**Fig. 2D**–**F**).

Subsequently, the selectivity and mode of action of the B7-H6/CD3 ITE was further characterized in *in vitro* coculture experiments with human T cells and B7-H6–positive HCT-15, or B7-H6–negative CHO-3E7 cell lines. The B7-H6/CD3 ITE-induced T cell–redirected lysis was strictly dependent on B7-H6 expression and $CD4^+$ as well as $CD8^+$ T cells contributed to the lysis activity (**Fig. 2G** and **H**). The potency and maximal lysis of the B7-H6/CD3 ITE-induced lysis of HCT-15 cells depended on the effector to target cell (E:T) ratio with lysis activity already observed at an E:T ratio of 1:5 and maximal lysis activity reached at an E:T ratio of ≥ 5:1 (**Fig. 2I**). Assessment of CD25, CD69, and CD107a expression on the cell surface of T cells, intracellular granzyme B in T cells, IFNγ and IL2 levels in the cell culture supernatant confirmed the B7-H6 dependency of the B7-H6/CD3 ITE (**Fig. 2J**–**L**). Further analysis confirmed the B7-H6–dependent induction of proliferation of T cells in presence of B7-H6–positive HCT-15 cells but not B7-H6–negative CHO-3E7 cells (**Fig. 2M**).

B7-H6/CD3 ITE monotherapy mediated antitumor activity and modulation of tumor-infiltrating T cells *in vivo*

In vivo B7-H6/CD3 ITE monotherapy studies were conducted in human B7-H6–positive HCT-15 xenograft bearing PBMC-humanized NSG or NCI-H716 xenograft bearing T cell–humanized NOG mouse models.

In a dose–response study in HCT-15 xenograft tumor-bearing PBMC-humanized NSG mice (**Fig. 3A**), B7-H6/CD3 ITE was administered at three doses (0.005, 0.05, 0.5 mg/kg, i.v.) in a every 7 days regimen and as a single dose. Dosing schedules were selected on the basis of the observed pharmacokinetic profile in a single dose (1 mg/kg, i.v.) study in non–tumor-bearing NOG mice, where the B7-H6/CD3 ITE exhibited a half-life of 10 days (Supplementary Fig. S4). Treatment with B7-H6/CD3 ITE in the every 7 days regimen led to 112% ($P < 0.0001$) tumor growth inhibition in the 0.5 mg/kg dose group with tumor regression in 6 of 7 mice, and 55% ($P < 0.0001$) tumor growth inhibition in the 0.05 mg/kg dose group. Administration as a single dose led to 100% ($P < 0.0001$) tumor growth inhibition with tumor regressions in 3 of 8 mice in the 0.5 mg/kg dose group at the study end on day 18 (**Fig. 3B**). In a second study, the influence of different PBMC donors was evaluated. In this study, HCT-15 tumor-bearing NSG mice were humanized with PBMCs isolated from three different donors and treated with 0.5 mg/kg B7-H6/CD3 ITE in a every 7 days regimen. Tumor growth inhibition at the end of the study on day 18 ranged from 93% in the group humanized with PBMCs from donor A to 111% in the group humanized with donor B. Tumor regressions also varied between the groups, ranging from 1 of 9 animals regressing in the group humanized with donor A and 9 of 9 animals regressing in the group humanized with donor B (**Fig. 3C**–**E**). At the end of the study on day 18, tumors from the group treated with donor A were harvested,

A

Colorectal cancer

Stage	# of cases	# of positive tumors (%)	# of negative tumors (%)
I	13	13 (26 %)	0
II	20	20 (40 %)	0
III	11	10 (20 %)	1 (2 %)
IV	6	6 (12 %)	0
total	**50**	**49 (98 %)**	**1 (2 %)**

B

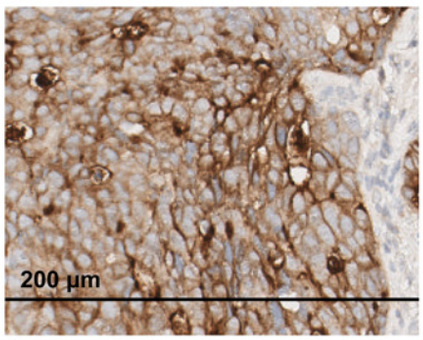

C

Gastric cancer

Stage	# of cases	# of positive tumors (%)	# of negative tumors (%)
I	2	2 (5 %)	0
II	14	11 (26 %)	3 (%)
III	18	14 (33 %)	4 (%)
IV	9	6 (14 %)	3 (7 %)
total	**43**	**33 (77 %)**	**10 (23 %)**

D

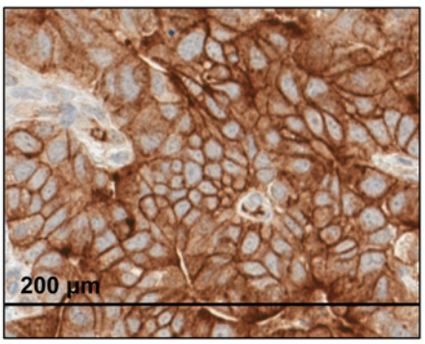

E

Pancreatic cancer

	# of cases	# of positive tumors (%)	# of negative tumors (%)
total	**46**	**29 (63 %)**	**17 (27 %)**

F

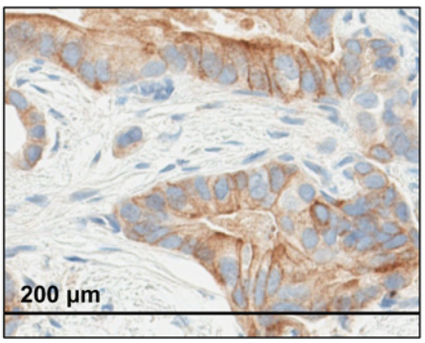

Figure 1.
Identification of B7-H6 as antigen in human gastrointestinal tumor tissues. **A-F,** Colorectal cancer (**A** and **B**), gastric cancer (**C** and **D**), and pancreatic cancer (**E** and **F**) tissues containing at least 1% tumor cells with membranous B7-H6 expression. Right, representative images of colorectal cancer (**B**), gastric cancer (**D**), and pancreatic cancer (**F**) tissue sections. Cells with membranous B7-H6 staining were quantified manually by a trained pathologist.

processed, and analyzed by flow cytometry for presence of tumor cells and infiltrating T cells. Treatment with B7-H6/CD3 ITE led to a statistically significant reduction of tumor weight, ($P < 0.0001$), tumor cells ($P < 0.05$), and an increase of tumor-infiltrating $CD8^+$ T cells ($P < 0.001$). Treatment also led to an increase of tumor-infiltrating $CD4^+$ T cells; however, this increase was not statistically significant (**Fig. 3F–I**).

In a subsequent study in NCI-H716 xenograft bearing T cell–humanized NOG mice (**Fig. 4A**), the B7-H6/CD3 ITE was administered at a dose of 0.05 mg/kg, i.v. in a weekly (every 7 days) regimen or as a single dose on day 1. Treatment with B7-H6/CD3 ITE in the every 7 days regimen led to sustained tumor regressions in all 9 animals on day 16 and 5 of 9 animals on day 28 (TGI = 105%, $P < 0.0001$). Treatment with B7-H6/CD3 ITE administered as single dose led to tumor regressions in 6 of 9 animals until day 22; however, tumor regrowth after day 22 was observed. At the end of the study (day 28), a statistically significant tumor growth inhibition (TGI = 79%, $P < 0.05$) with 1 animal still in regression was observed (**Fig. 4B**). B7-H6/CD3 ITE plasma levels in NCI-H716 xenograft tumor-bearing T cell–humanized NOG mice were confirmed after administration of 0.05 mg/kg, i.v. in a every 7 days regimen or as a single dose (**Fig. 4C**).

In a separate study, we further assessed the ability of the B7-H6/CD3 ITE to modulate the inflammatory environment in the NCI-H716 xenograft tumor-bearing T cell–humanized mice. NCI-H716 xenograft tumor tissues from animals were collected one day after administration of one dose of 0.05 mg/kg B7-H6/CD3 ITE i.v., and sections of FFPE tissues were immunohistochemically stained with anti-CD3, anti-CD69, anti-granzyme B, anti-perforin, anti-PD-L1, and anti-cC3 (cleaved caspase 3) antibodies. A statistically significant increase in tumor-infiltrating $CD3^+$ T cells (**Fig. 4D** and **J**; $P < 0.001$) in B7-H6/

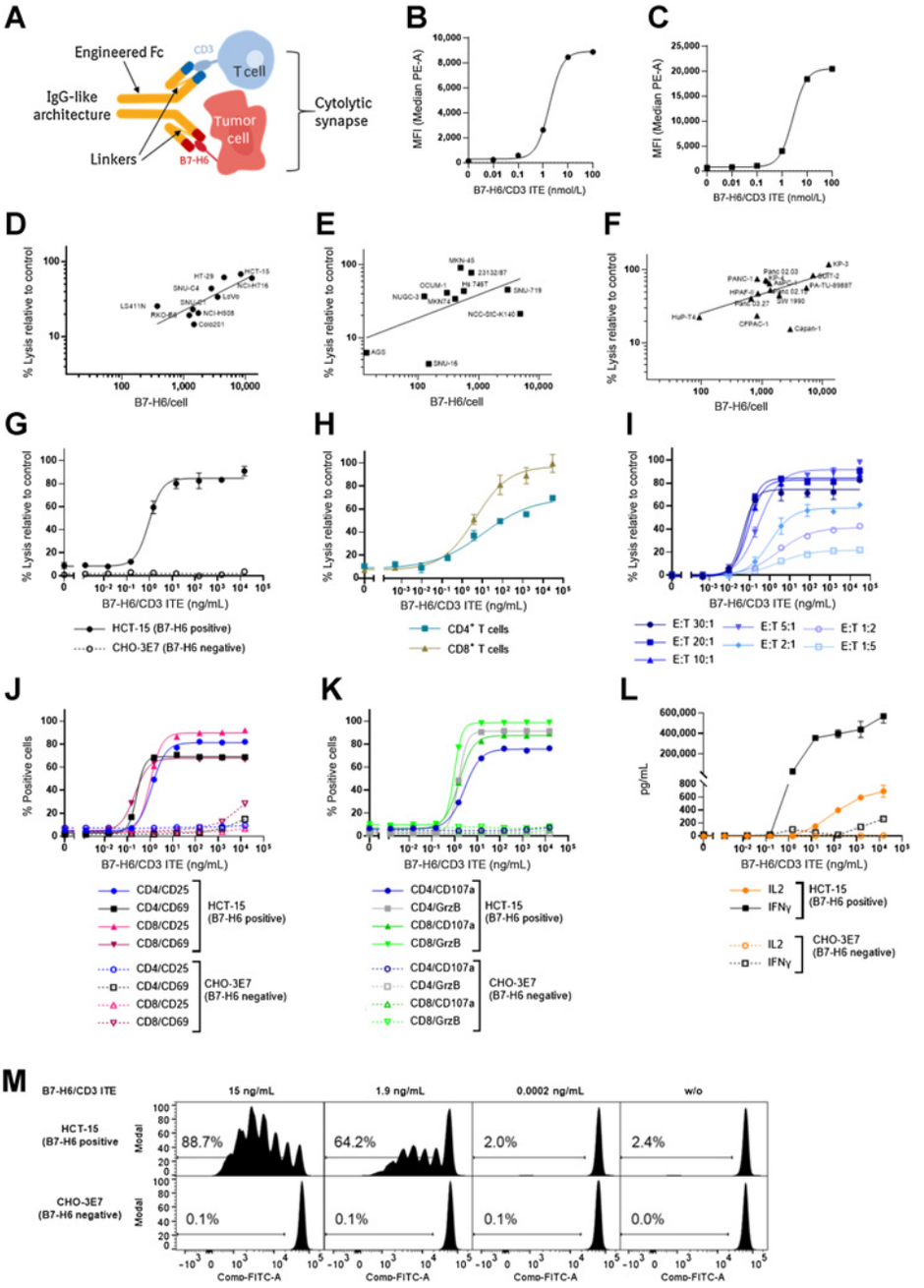

Figure 2.

In *vitro* mode of action of B7-H6/CD3 ITE. **A,** Schematic graphic of B7-H6/CD3 ITE. **B** and **C,** Binding to HCT-15 (**B**) and T cells (**C**). Each datapoint represents a single measurement. **D-F,** Correlation of B7-H6 cell surface density and B7-H6/CD3 ITE-induced lysis of 10 colorectal (**D**), 10 gastric (**E**), and 14 pancreatic (**F**) cancer cell lines incubated with T cells in a ratio of 1:10 in the presence of 1.5 µg/mL B7-H6/CD3 ITE for 72 hours. **G–M,** Human T cells and B7-H6–positive HCT-15 cells or B7-H6–negative CHO-3E7 cells were cocultivated in the presence of increasing concentrations of B7-H6/CD3 ITE for 72 hours. **G,** B7-H6 dependency of B7-H6/CD3 ITE-induced cell lysis [effector to target cell ratio (E:T) 10:1]. **H,** B7-H6/CD3-induced lysis of HCT-15 cells by $CD4^+$ and $CD8^+$ T cells (E:T 10:1). **I,** E:T ratio dependency of B7-H6/CD3 ITE-induced lysis of HCT-15 cells. **J,** B7-H6 dependency of B7-H6/CD3 ITE-induced upregulation of CD25 and CD69 on $CD4^+$ and $CD8^+$ T cells (E:T 10:1). **K,** B7-H6 dependency of B7-H6/CD3 ITE-induced upregulation of extracellular CD107a and intracellular granzyme B (GrzB) in $CD4^+$ and $CD8^+$ T cells (E:T 10:1). **L,** B7-H6 dependency of B7-H6/CD3 ITE-induced secretion of IL2 and IFNγ by T cells (E:T 10:1). **M,** B7-H6 dependency of B7-H6/CD3 ITE-induced proliferation of T cells (E:T 10:1) after 6 days of coculture. Each datapoint represents a single measurement. For **G, H, I,** and **L,** each datapoint represents the mean of duplicates, error bars represent the SD. For **J** and **K,** each datapoint represents data from duplicates which were pooled for the flow cytometry analysis.

CD3 ITE-treated animals compared with the vehicle-treated animals was observed, which correlates with the increase of cleaved caspase 3 (**Fig. 4E** and **J**) in the tumor cells. Tumor-infiltrating T cells were activated as confirmed by upregulation of CD69, perforin, and granzyme B (**Fig. 4F–H**, and J). As a result of the presence of activated T cells and resulting inflamed tumor environment, expression of PD-L1 was upregulated (**Fig. 4I** and **J**).

Combination with anti-PD-1 enhances the antitumor activity of B7-H6/CD3 ITE

To further evaluate the potential effect of upregulation of the PD-(L)1 pathway on the B7-H6/CD3 ITE activity, we generated a recombinant PD-L1–overexpressing HCT-15-PD-L1 cell line that expressed 120,000 PD-L1 molecules per cell. The parental (PD-L1–negative) HCT-15 cell line and the recombinant HCT-15-PD-L1 cell line had comparable B7-H6 expression levels (**Fig. 5A**). In an *in vitro* cytotoxicity assay, the B7-H6/CD3 ITE-induced lysis of HCT-15-PD-L1 cells was slightly lower than of PD-L1–negative HCT-15 cells (100% vs. 80% lysis). While combination with anti-PD-1 slightly increased the B7-H6/CD3 ITE-induced lysis of the PD-L1–overexpressing HCT-15-PD-L1 cells (90% lysis), the combination did not have any effect on PD-L1–negative HCT-15 cells (**Fig. 5B**).

While in the NCI-H716 tumor model, the endogenous PD-L1 expression levels, which were induced one day after with the B7-H6/

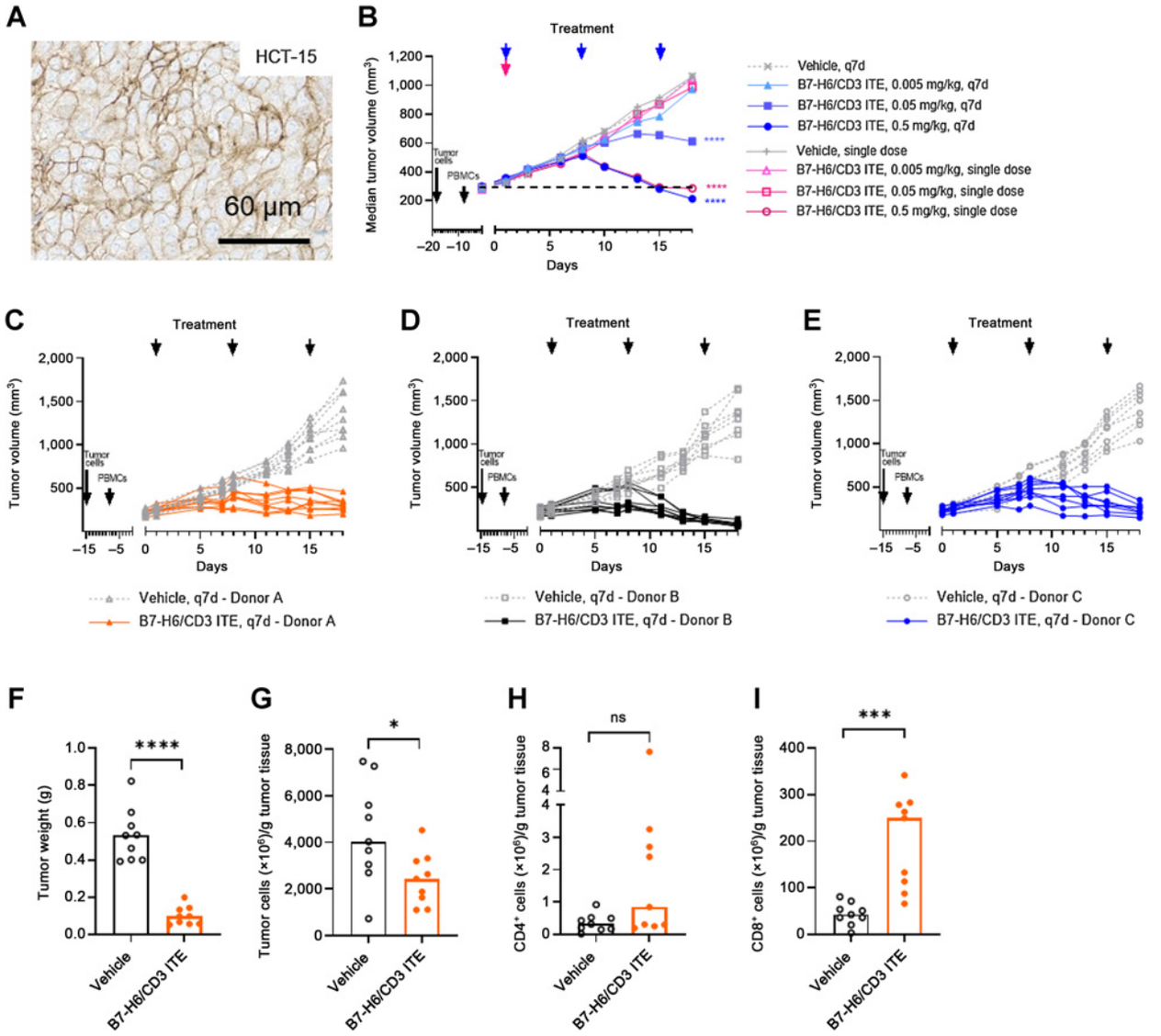

Figure 3.

B7-H6/CD3 ITE monotherapy induces antitumor activity in human HCT-15 xenograft tumor bearing PBMC humanized *in vivo* mouse model. **A** and **B,** B7-H6 IHC (**A**), dose and schedule dependency (**B**). Each datapoint represents the median of 8 animals. **C–E,** Donor dependency of antitumor activity of B7-H6/CD3 ITE. Each datapoint represents 1 animal. **F-I,** Flow cytometry analysis of HCT-15 xenograft tumors (PBMC donor A) on day 18, tumor weight (**F**), number of tumor cells (**G**), number of $CD4^+$ T cells (**H**), and number of $CD8^+$ T cells (**I**) per gram tumor tissue. Each datapoint represents one animal, and bars represent the median. ****, $P < 0.0001$; ***, $P < 0.001$; **, $P < 0.01$; *, $P < 0.05$.

CD3 ITE, did not lead to abrogation of the antitumor efficacy, the PD-L1 overexpression on recombinant HCT-15-PD-L1 cells influenced the antitumor activity. In HCT-15-PD-L1 xenograft (**Fig. 5C**) bearing PBMC-humanized NSG mice, anti-PD-1 or B7-H6/CD3 ITE administered as monotherapies did not exhibit antitumor activity; however, the combination therapy of B7-H6/CD3 ITE and anti-PD-1 led to tumor regression in all treated animals (**Fig. 5** D–F).

Activity of B7-H6/CD3 ITE in *ex vivo* patient-derived colorectal cancer precision cut tumor slice cultures

To assess the activity of the B7-H6/CD3 ITE in human colorectal cancer tissues with endogenous expression levels of B7-H6 on tumor cells and tumor-infiltrating T cells, we incubated colorectal cancer tissue slices from 10 patients with colorectal cancer, 9 with microsatellite stable and, one with high microsatellite instability status, for 48 hours in presence of 15 µg/mL B7-H6/CD3 ITE or medium alone (untreated) before quantifying cytokines in the cell culture supernatant. Treatment with B7-H6/CD3 ITE induced secretion of IFNγ (5- to 700-fold increase), IP-10 (10- to 500-fold increase), and IL2 (10- to 500-fold increase) by tumor-infiltrating immune cells in all 10 analyzed colorectal cancer tissue slices. The combination with anti-PD-1 further increased the secretion of IFNγ in nine of 10, and IL2 and IP-10 in eight of 10 colorectal cancer tissue slices (1.1- to 2.9-fold increase on top of B7-H6/CD3

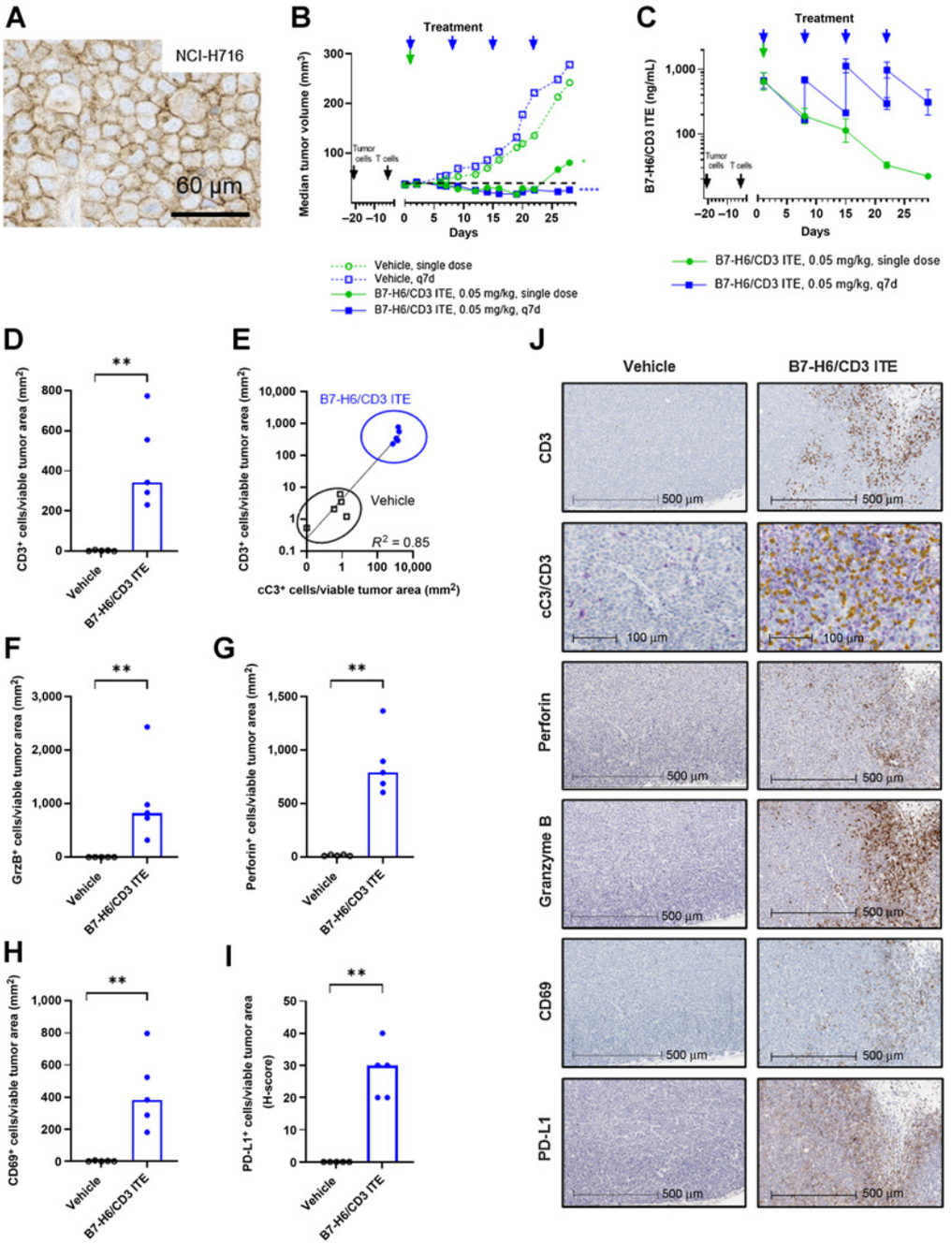

Figure 4.

B7-H6/CD3 ITE monotherapy induces antitumor activity and modulation of tumor-infiltrating T cells in human NCI-H716 xenograft tumor-bearing T cell–humanized *in vivo* mouse model. **A** and **B,** B7-H6 IHC (**A**), and antitumor activity (**B;** each datapoint represents the median of 9 animals). **C,** Pharmacokinetic profile (each datapoint represents the mean of 3 animals, error bars represent the SD). **D–J,** IHC analysis of NCI-H716 xenograft tumors on day 2 for CD3 (**D**), cC3 (purple) and CD3 (yellow; **E**), GrzB (**F**), perforin (**G**), CD69 (**H**), and PD-L1 (**I**). **J,** Representative IHC stainings. **D** and **F–I,** Each datapoint represents 1 animal, bars represent the median. ****, $P < 0.0001$; ***, $P < 0.001$; **, $P < 0.01$; *, $P < 0.05$.

monotherapy treatment; **Fig. 6A–C**). For retrospective analysis of B7-H6 expression on tumor cells and presence of T cells, a fresh tumor tissue slice was reserved at baseline, fixed in formalin for further analysis of B7-H6 and CD3 expression by IHC. B7-H6 expression and presence of $CD3^+$ T cells was confirmed retrospectively in all 10 colorectal cancer tissue samples. Expression of B7-H6 covered a similar range (H-scores between 1 and 140) as in the analyzed colorectal cancer tissues in the prevalence study (**Figs. 6D** and **E**).

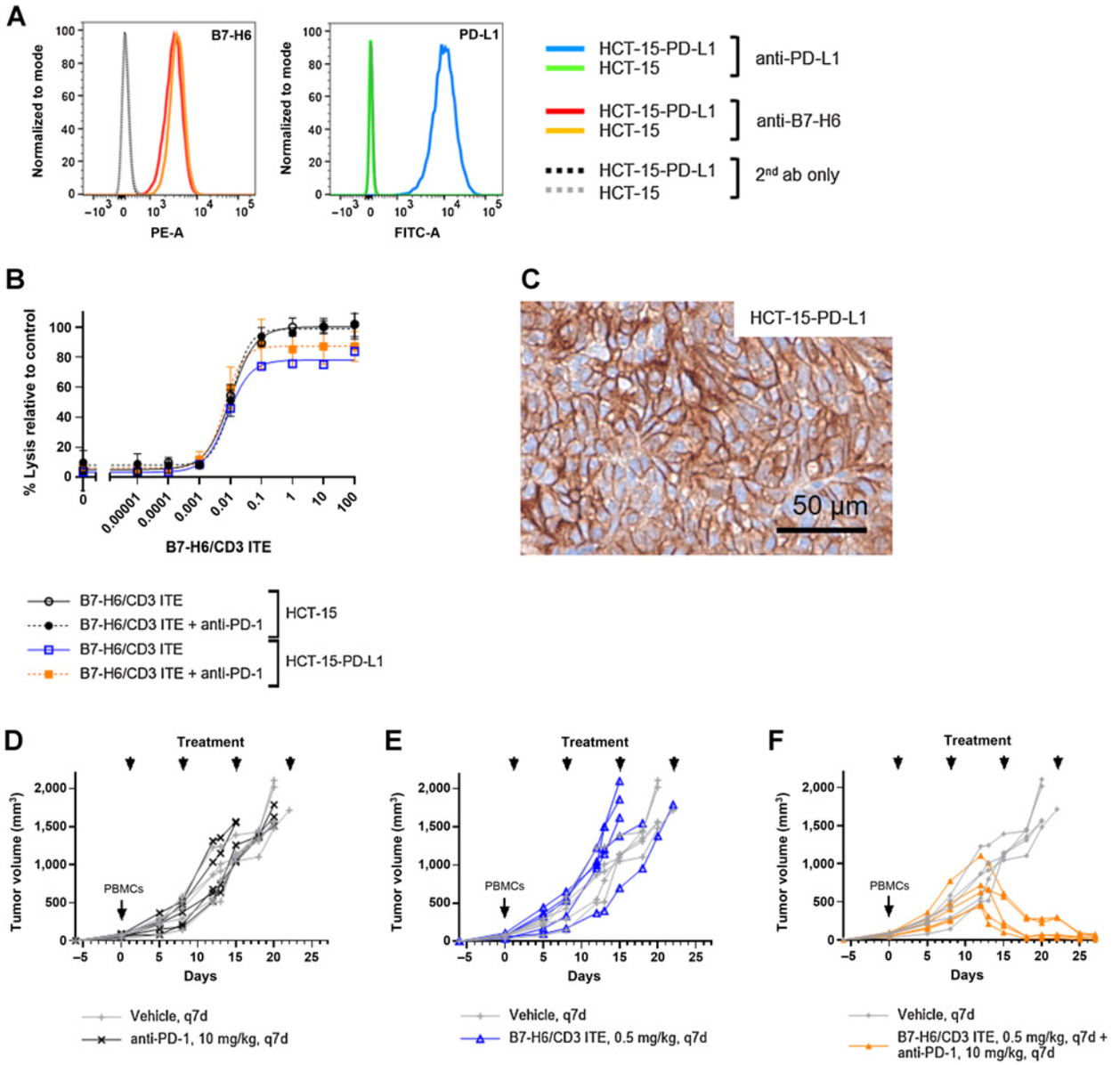

Figure 5.

Combination with anti-PD-1 enhances antitumor activity of B7-H6/CD3 ITE. **A,** B7-H6 and PD-L1 expression on parental HCT-15 and recombinant HCT-15-PD-L1 cell lines. **B,** B7-H6/CD3 ITE-induced cell lysis (E:T 10:1, 72 hours) *in vitro*. Each datapoint represents the mean of duplicates, error bars represent the SD. **C,** PD-L1 expression in HCT-15-PD-L1 xenograft tissue. **D-F,** Antitumor activity of anti-PD-1 monotherapy (**D**), B7-H6/CD3 ITE monotherapy (**E**), and B7-H6/CD3 ITE and anti-PD-1 combination therapy (**F**) in HCT-15-PD-L1 xenograft bearing PBMC-humanized mouse model.

Discussion

Advanced-stage colorectal, gastric, and pancreatic cancer represent tumor indications with high unmet medical need. Immunomodulating therapies, for example, anti-PD-1 inhibitors, remain mainly ineffective due to the immunosuppressive tumor environment (32–36) and the identification of tumor-specific antigens to ensure a therapeutic window remains a key challenge, as observed in phase I clinical trials with solitomab (EpCAM targeting BiTE) and MEDI-565 (CEA targeting BiTE), where toxicities due to normal tissue expression were observed (18–21).

In this article, we describe the preclinical antitumor activity of a novel B7-H6–targeted T cell–engaging antibody for the treatment of colorectal, gastric, and pancreatic cancer tissues. Initially, B7-H6 was identified as a cell surface molecule that is absent in normal tissues but expressed on leukemia and lymphoma cells which binds to NKp30 on NK cells and triggers the NK-cell cytotoxicity against these cells (22). Another *in vitro* study with cancer cell lines suggests that B7-H6 mRNA and protein expression may be upregulated under cellular stress conditions induced by chemotherapy (cisplatin, 5-fluorouracil), radiotherapy, nonlethal heat shock, and TNFα treatment (37). In our cancer tissue analysis, we detected B7-H6 expression in 98% of

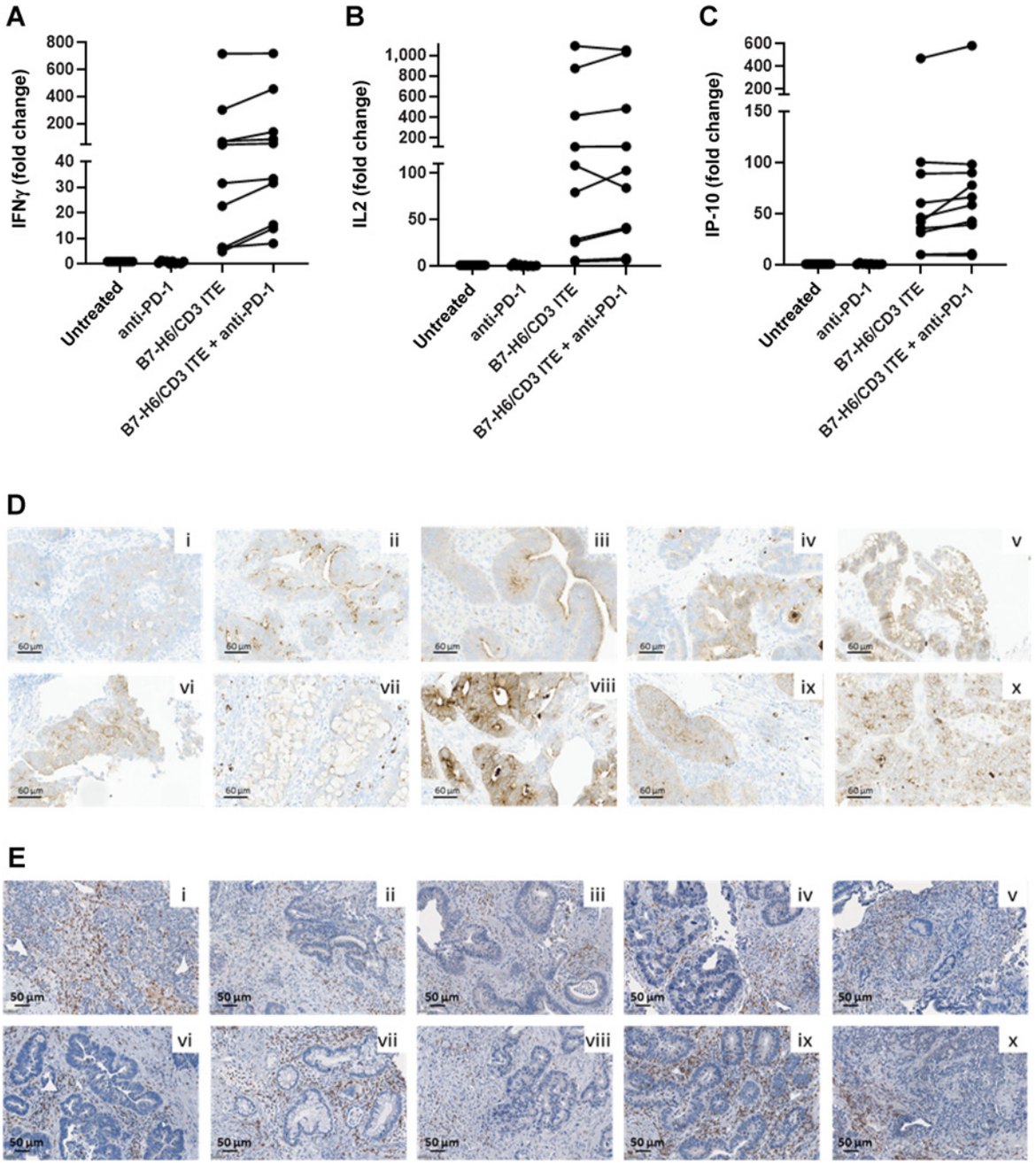

Figure 6.

B7-H6/CD3 ITE induces secretion of cytokines in colorectal cancer precision cut tumor slice cultures. **A–C,** Fresh tumor tissue from 10 patients with colorectal cancer were cultured for 48 hours in a 24-well plate in presence of 15 µg/mL B7-H6/CD3 ITE and/or 10 µg/mL anti-PD-1 or medium alone (untreated). IL2, IFNγ, and IP-10 were quantified in the cell culture supernatant. Each datapoint represents one tumor sample. **D** and **E,** B7-H6 (**D**) and CD3 (**E**) expression in 10 colorectal cancer tissue samples at baseline.

colorectal cancer, 77% of gastric cancer, and 63% of pancreatic cancer samples by IHC and confirmed the absence of B7-H6 membrane expression in nontumorous (normal) tissues using membrane proteomics, which suggests B7-H6 as an ideal target antigen for a tumor-selective targeting approach. B7-H6 expression has also been previously described in tumor tissues of patients with non–small cell lung cancer (38), small cell lung cancer (39), oral squamous cell cancer (40), and cervical cancer (41), providing the potential for a B7-H6–targeted therapeutic approach in a broad range of solid tumor indications. Further analysis of B7-H6 expression and correlation with more clinicopathologic features is still required to better characterize the B7-H6–positive patient population.

To target B7-H6, we have designed a novel half-life extended T cell–engaging bispecific antibody targeting B7-H6. The B7-H6/CD3 ITE is clearly differentiated to the short half-life B7-H6 BiTE (42) and B7-H6 CAR T cells (43–45), but also to recently described half-life extended T cell–engaging antibodies GUCY2 (8) and CEA TCB (6). B7-H6/CD3 ITE induces potent T cell–redirected lysis of B7-H6–positive colorectal, gastric, and pancreatic cancer cell lines by redirecting T cells toward B7-H6–postitive cancer cells without lysing B7-H6–negative target cells. As a result of the formation of the cytolytic synapse, T cells secrete proinflammatory cytokines and proliferate. *In vivo*, the B7-H6/CD3 ITE induced dose-dependent antitumor activity in subcutaneous colorectal cancer (NCI-H716, HCT-15) xenograft tumor-bearing PBMC or T cell–humanized mice. A single dose of B7-H6/CD3 ITE led to profound infiltration of T cells into the tumor tissue, and tumor regressions were observed with single doses of ≤ 0.5 mg/kg, which highlights the potential of the B7-H6/CD3 ITE for treatment of noninflamed tumors, which are currently difficult to treat with available immunotherapies. As a result of the inflamed tumor environment induced by treatment with the B7-H6/CD3 ITE, the tumor cells upregulated PD-L1 expression already one day after treatment initiation. Although, the B7-H6/CD3 ITE-treatment related upregulation of endogenous PD-L1 did not result in abrogation of the antitumor efficacy in this study, further studies using a mechanistic *in vivo* model with recombinant and highly PD-L1–overexpressing tumors showed that overexpression of PD-L1 may influence the antitumor activity of the B7-H6/CD3 ITE, and combination with anti-PD-1 inhibitors may provide potential for enhanced antitumor efficacy and may sensitize tumors to anti-PD-1 treatment. In future studies, it will be important to further characterize the combination in *in vivo* models with endogenous PD-L1 expression levels. *In vitro* coculture assays as well as humanized xenograft mouse models based on human cancer cell lines and PBMCs or T cells isolated from healthy blood donors represent good tools for initial characterization of T-cell engagers; however, these models can only represent isolated features of the complex human cancer tissue. Precision cut tumor slice cultures represent a primary human disease relevant model system which recapitulates the tissue architecture including its tumor cells, microenvironment, and infiltrating immune cells, and is to date the closest human cancer model system. Importantly, the B7-H6/CD3 ITE induces secretion of cytokines in human colorectal cancer tissue slices demonstrating the ability to redirect tumor-infiltrating T cells toward colorectal cancer cells with endogenous B7-H6 expression levels.

Taken together, the B7-H6/CD3 ITE provides a novel drug candidate for the treatment of gastrointestinal tumors with upside potential in other B7-H6–expressing solid tumor types, which is currently being investigated in a nonrandomized, open-label, dose-escalation trial (NCT04752215) as monotherapy and in combination with the anti-PD-1 antibody ezabenlimab.

Authors' Disclosures

W. Zhang reports personal fees from Boehringer Ingelheim during the conduct of the study. Y.-H. Lin reports personal fees from Boehringer Ingelheim during the conduct of the study. L. Yang reports personal fees from Boehringer Ingelheim during the conduct of the study. F. Sayedian reports personal fees from Boehringer Ingelheim during the conduct of the study. M. Fabits reports grants from Boehringer Ingelheim during the conduct of the study; and grants from Boehringer Ingelheim outside the submitted work. M. Bergmann reports grants and personal fees from Boehringer Ingelheim during the conduct of the study; grants from Bristol Myers Squibb and Boehringer Ingelheim; and personal fees from Bristol Myers Squibb outside the submitted work. L. Corrales reports grants from the Austrian Research Promotion Agency (Basisprogramm grants, FFG; 860968, 869530, 875923, and 883369) during the conduct of the study; and L. Corrales is a full-time employee of Boehringer Ingelheim affiliates. A.B. Vogt reports personal fees from Boehringer Ingelheim during the conduct of the study. L.J. Hudson reports personal fees from Oxford BioTherapeutics Ltd during the conduct of the study; and other support from Boehringer Ingelheim outside the submitted work. M.P. Barnes reports personal fees from Oxford Biotherapeutics Ltd during the conduct of the study; and other support from Boehringer Ingelheim outside the submitted work. V. Voynov reports personal fees from Boehringer Ingelheim during the conduct of the study; in addition, V. Voynov has a patent for Multi-specific binding proteins for cancer treatment pending. P.J. Adam reports personal fees from Boehringer Ingelheim and grants from Basisprogramm grants of the Austrian Research Promotion Agency during the conduct of the study; in addition, P.J. Adam has a patent for Multi-specific binding proteins for cancer treatment pending. S. Hipp reports personal fees from Boehringer Ingelheim Pharmaceuticals, Inc. and grants from Basisprogramm grants of the Austrian Research Promotion Agency during the conduct of the study; in addition, S. Hipp has a patent for Multi-specific binding proteins for cancer treatment pending. No disclosures were reported by the other authors.

Authors' Contributions

W. Zhang: Conceptualization, supervision, visualization, methodology, writing–original draft, writing–review and editing. **A. Auguste:** Formal analysis, supervision, methodology. **X. Liao:** Supervision, methodology. **C. Walterskirchen:** Methodology. **K. Bauer:** Methodology. **Y.-H. Lin:** Methodology. **L. Yang:** Methodology. **F. Sayedian:** Validation, methodology. **M. Fabits:** Methodology. **M. Bergmann:** Methodology. **C. Binder:** Methodology. **L. Corrales:** Methodology, writing–review and editing. **A.B. Vogt:** Supervision, methodology, writing–review and editing. **L.J. Hudson:** Methodology. **M.P. Barnes:** Methodology. **A. Bisht:** Methodology. **C. Giragossian:** Supervision, visualization, methodology, writing–review and editing. **V. Voynov:** Supervision, methodology. **P.J. Adam:** Funding acquisition, writing–review and editing. **S. Hipp:** Conceptualization, data curation, formal analysis, supervision, funding acquisition, visualization, methodology, writing–original draft, writing–review and editing.

Acknowledgments

We thank Richard Liedauer, Margit Urban, Katharina Martin, Ilse Apfler, Irene Schweiger, Eric Bolella, and Carolina Klicka for their experimental support and help for this study, all colleagues from Biotherapeutics Discovery for providing the molecule, and Paolo Chetta for support in histologic analysis of colorectal cancer samples in *ex vivo* studies.

This study was supported by Boehringer Ingelheim and the Basisprogramm grants of the Austrian Research Promotion Agency (FFG; 860968, 869530, 875923, and 883369).

The publication costs of this article were defrayed in part by the payment of publication fees. Therefore, and solely to indicate this fact, this article is hereby marked "advertisement" in accordance with 18 USC section 1734.

Note

Supplementary data for this article are available at Clinical Cancer Research Online (http://clincancerres.aacrjournals.org/).

Received July 6, 2022; revised August 22, 2022; accepted September 22, 2022; published first September 27, 2022.

References

1. Colorectal cancer Fact Sheet (Globocan 2020) [Internet]. International Agency for Research on Cancer, World Health Organization. Available from: https://gco.iarc.fr/today/data/factsheets/cancers/10_8_9-Colorectum-fact-sheet.pdf.
2. Pancreas Cancer Fact Sheet (Globocan 2020) [Internet]. International Agency for Research on Cancer, World Health Organization. Available from: https://gco.iarc.fr/today/data/factsheets/cancers/13-Pancreas-fact-sheet.pdf.

3. Stomach Cancer Fact Sheet (Globocan 2020) [Internet]. International Agency for Research on Cancer, World Health Organization. Available from: https://gco.iarc.fr/today/data/factsheets/cancers/7-Stomach-fact-sheet.pdf.
4. Gruen M, Bommert K, Bargou RC. T-cell-mediated lysis of B cells induced by a CD19xCD3 bispecific single-chain antibody is perforin dependent and death receptor independent. Cancer Immunol Immunother 2004;53:625–32.
5. Hoffmann P, Hofmeister R, Brischwein K, Brandl C, Crommer S, Bargou R, et al. Serial killing of tumor cells by cytotoxic T cells redirected with a CD19-/CD3-bispecific single-chain antibody construct. Int J Cancer 2005;115:98–104.
6. Bacac M, Fauti T, Sam J, Colombetti S, Weinzierl T, Ouaret D, et al. A novel carcinoembryonic antigen T-cell bispecific antibody (CEA TCB) for the treatment of solid tumors. Clin Cancer Res 2016;22:3286–97.
7. Hipp S, Tai Y-T, Blanset D, Deegen P, Wahl J, Thomas O, et al. A novel BCMA/CD3 bispecific T-cell engager for the treatment of multiple myeloma induces selective lysis *in vitro* and *in vivo*. Leukemia 2017;31:1743–51.
8. Mathur D, Root AR, Bugaj-Gaweda B, Bisulco S, Tan X, Fang W, et al. A novel GUCY2C-CD3 T-cell engaging bispecific construct (PF-07062119) for the treatment of gastrointestinal cancers. Clin Cancer Res 2020;26:2188–202.
9. Hipp S, Voynov V, Drobits-Handl B, Giragossian C, Trapani F, Nixon AE, et al. A bispecific DLL3/CD3 IgG-like T-cell engaging antibody induces antitumor responses in small cell lung cancer. Clin Cancer Res 2020;26:5258–68.
10. Sanford M. Blinatumomab: first global approval. Drugs 2015;75:321–7.
11. Topp MS, Duell J, Zugmeier G, Attal M, Moreau P, Langer C, et al. Anti–B-cell maturation antigen BiTE molecule AMG 420 induces responses in multiple myeloma. J Clin Oncol 2020;38:775–83.
12. Junttila TT, Li J, Johnston J, Hristopoulos M, Clark R, Ellerman D, et al. Antitumor efficacy of a bispecific antibody that targets HER2 and activates T cells. Cancer Res 2014;74:5561–71.
13. Tabernero J, Melero I, Ros W, Argiles G, Marabelle A, Rodriguez-Ruiz ME, et al. Phase Ia and Ib studies of the novel carcinoembryonic antigen (CEA) T-cell bispecific (CEA CD3 TCB) antibody as a single agent and in combination with atezolizumab: preliminary efficacy and safety in patients with metastatic colorectal cancer (mCRC). J Clin Oncol 35: 15s, 2017 (supl; abstr 3002).
14. Giffin MJ, Cooke K, Lobenhofer EK, Estrada J, Zhan J, Deegen P, et al. AMG 757, a half-life extended, DLL3-targeted bispecific T-cell engager, shows high potency and sensitivity in preclinical models of Small-cell lung cancer. Clin Cancer Res 2021;27:1526–37.
15. Deegen P, Thomas O, Nolan-Stevaux O, Li S, Wahl J, Bogner P, et al. The PSMA-targeting Half-life extended BiTE therapy AMG 160 has potent antitumor activity in preclinical models of metastatic castration-resistant prostate cancer. Clin Cancer Res 2021;27:2928–37.
16. Zekri L, Vogt F, Osburg L, Müller S, Kauer J, Manz T, et al. An IgG-based bispecific antibody for improved dual targeting in PSMA-positive cancer. Embo Mol Med 2021;13:e11902.
17. Nathan P, Hassel JC, Rutkowski P, Baurain J-F, Butler MO, Schlaak M, et al. Overall survival benefit with tebentafusp in metastatic uveal melanoma. New Engl J Med 2021;385:1196–206.
18. Kebenko M, Goebeler M-E, Wolf M, Hasenburg A, Seggewiss-Bernhardt R, Ritter B, et al. A multicenter phase 1 study of solitomab (MT110, AMG 110), a bispecific EpCAM/CD3 T-cell engager (BiTE®) antibody construct, in patients with refractory solid tumors. Oncoimmunology 2018;7:e1450710.
19. Schmelzer E, Reid LM. EpCAM expression in normal, non-pathological tissues. Front Biosci 2008;13:3096–100.
20. Pishvaian M, Morse MA, McDevitt J, Norton JD, Ren S, Robbie GJ, et al. Phase 1 dose escalation study of MEDI-565, a bispecific T-cell engager that targets human carcinoembryonic antigen, in patients with advanced gastrointestinal adenocarcinomas. Clin Colorectal Cancer 2016;15:345–51.
21. Hammarström S. The carcinoembryonic antigen (CEA) family: structures, suggested functions and expression in normal and malignant tissues. Semin Cancer Biol 1999;9:67–81.
22. Brandt CS, Baratin M, Yi EC, Kennedy J, Gao Z, Fox B, et al. The B7 family member B7-H6 is a tumor cell ligand for the activating natural killer cell receptor NKp30 in humans. J Exp Med 2009;206:1495–503.
23. Li Y, Wang Q, Mariuzza RA. Structure of the human activating natural cytotoxicity receptor NKp30 bound to its tumor cell ligand B7-H6. J Exp Med 2011;208:703–14.
24. Xu X, Li Y, Gauthier L, Chen Q, Vivier E, Mariuzza RA. Expression, crystallization and X-ray diffraction analysis of a complex between B7-H6, a tumor cell ligand for the natural cytotoxicity receptor NKp30, and an inhibitory antibody. Acta Crystallogr Sect F Struct Biology Commun 2015;71:697–701.
25. Zettl M, Wurm M, Schaaf O, Tirapu I, Mostböck S, Reschke M, et al. *In vitro* and *in vivo* characterization of the PD-1 targeting antibody BI 754091 [abstract]. In: Proceedings of the American Association for Cancer Research Annual Meeting 2018; 2018 Apr 14–18; Chicago, IL. Philadelphia (PA): AACR; Cancer Res 2018;78(13 Suppl):Abstract nr 4558.
26. Spigel D, Falchook G, Patel M, Bashir B, Ulahannan S, Duffy C, et al. A first-in-human phase I dose-escalation trial of the B7-H6/CD3 T-cell engager BI 765049 ± ezabenlimab (BI 754091) in patients with advanced solid tumors expressing B7-H6. J Immunother Cancer 2021; A510.
27. Rohlff C, Stamps A. Ephrin type-a receptor 10 protein. WO2009087462A2; 2007.
28. Rohlff C. New approaches towards integrated proteomic databases and depositories. Expert Rev Proteomic 2014;1:267–74.
29. Singh S, Kroe-Barrett RR, Canada KA, Zhu X, Sepulveda E, Wu H, et al. Selective targeting of the IL23 pathway: generation and characterization of a novel high-affinity humanized anti-IL23A antibody. Mabs 2015;7:778–91.
30. Pessano S, Oettgen H, Bhan AK, Terhorst C. The T3/T cell receptor complex: antigenic distinction between the two 20-kd T3 (T3-delta and T3-epsilon) subunits. EMBO J 1985;4:337–44.
31. Venkataramani S, Low S, Weigle B, Dutcher D, Jerath K, Menzenski M, et al. Design and characterization of zweimab and doppelmab, high affinity dual antagonistic anti-TSLP/IL13 bispecific antibodies. Biochem Biophys Res Commun 2018;504:19–24.
32. Werner J, Heinemann V. Standards and challenges of care for colorectal cancer today. Visc Med 2016;32:156–7.
33. Holch J, Stintzing S, Heinemann V. Treatment of metastatic colorectal cancer: standard of care and future perspectives. Visc Med 2016;32:178–83.
34. Orditura M, Galizia G, Sforza V, Gambardella V, Fabozzi A, Laterza MM, et al. Treatment of gastric cancer. World J Gastroenterol 2014;20:1635–49.
35. Mohammad AA. Advanced pancreatic cancer: the standard of care and new opportunities. Oncol Rev 2018;12:370.
36. Herbst RS, Soria J-C, Kowanetz M, Fine GD, Hamid O, Gordon MS, et al. Predictive correlates of response to the anti-PD-L1 antibody MPDL3280A in cancer patients. Nature 2014;515:563–7.
37. Cao G, Wang J, Zheng X, Wei H, Tian Z, Sun R. Tumor therapeutics work as stress inducers to enhance tumor sensitivity to natural killer (NK) cell cytolysis by up-regulating NKp30 ligand B7-H6^{+}. J Biol Chem 2015;290:29964–73.
38. Zhang X, Zhang G, Qin Y, Bai R, Huang J. B7-H6 expression in non-small cell lung cancers. Int J Clin Exp Pathol 2014;7:6936–42.
39. Thomas PL, Groves SM, Zhang Y-K, Li J, Gonzalez-Ericsson P, Sivagnanam S, et al. Beyond programmed death-ligand 1: B7-H6 emerges as a potential immunotherapy target in SCLC. J Thorac Oncol 2021;16:1211–23.
40. Wang J, Jin X, Liu J, Zhao K, Xu H, Wen J, et al. The prognostic value of B7-H6 protein expression in human oral squamous cell carcinoma. J Oral Pathol Med 2017;46:766–72.
41. Gutierrez-Silerio GY, Franco-Topete RA, Haramati J, Navarrete-Medina EM, Gutierrez-Franco J, Bueno-Topete MR, et al. Positive staining of the immunoligand B7-H6 in abnormal/transformed keratinocytes consistently accompanies the progression of cervical cancer. BMC Immunol 2020;21:9.
42. Wu M-R, Zhang T, Gacerez AT, Coupet TA, DeMars LR, Sentman CL. B7H6-specific bispecific T cell engagers lead to tumor elimination and host antitumor immunity. J Immunol 2015;194:5305–11.
43. Wu M-R, Zhang T, DeMars LR, Sentman CL. B7H6-specific chimeric antigen receptors lead to tumor elimination and host anti-tumor immunity. Gene Ther 2015;22:675–84.
44. Gacerez AT, Hua CK, Ackerman ME, Sentman CL. Chimeric antigen receptors with human scFvs preferentially induce T cell anti-tumor activity against tumors with high B7H6 expression. Cancer Immunol Immunother 2018;67:749–59.
45. Hua CK, Gacerez AT, Sentman CL, Ackerman ME. Development of unique cytotoxic chimeric antigen receptors based on human scFv targeting B7H6. Protein Eng Des Sel 2017;30:713–21.<./bib>